Water Research 220 (2022) 118656

Contents lists available at ScienceDirect

Water Research

journal homepage: www.elsevier.com/locate/watres

Integrated effects of polymer type, size and shape on the sinking dynamics of biofouled microplastics

Siguang Liu [a,b,1], Yifeng Huang [a,c,1], Dehua Luo [a], Xiao Wang [a], Zhenfeng Wang [a], Xiaoliang Ji [a], Zheng Chen [a], Randy A. Dahlgren [a,d], Minghua Zhang [a,d], Xu Shang [a,*]

[a] Key Laboratory of Watershed Sciences and Health of Zhejiang Province, School of Public Health and Management, Wenzhou Medical University, Wenzhou 325035, China
[b] Fujian Institute of Oceanography, Xiamen 361013, China
[c] State Key Laboratory of Marine Environmental Science, Xiamen University, Xiamen 361102, China
[d] Department of Land, Air and Water Resources, University of California Davis, CA 95616, USA

ARTICLE INFO

Keywords:
Microplastics
Biofouling
Sinking
Size and shape
Transport and fate

ABSTRACT

Sinking of microplastics (MPs) after biofouling is considered an important mechanisms responsible for the downward transport/sedimentation of MPs in the ocean and freshwaters. Previous studies demonstrated MP sinking caused by an increase in the composite density of MPs after biofouling, while MPs with smaller size or shapes with higher surface area to volume ratios (SA:V), such as films, are speculated to sink faster. In this study, we designed an *in situ* microcosm to simulate the ambient environmental conditions experienced by floating MPs to elucidate the biofouling and sinking of polyethylene (PE), polypropylene (PP), and expanded-polystyrene (EPS) MPs of various sizes and shapes. Our results showed smaller PE and PP MP granules sank faster than large ones. Even EPS granules of 100 μm diameter, having a much lower density (0.02 mg/mm^3) than water, started to sink after 2 weeks of biofouling. Moreover, PE film and fiber MPs with higher SA:V did not sink faster than PE MP granules of the same mass, implying that mechanisms other than SA:V, such as fouling contact area and drag coefficient, play a role in the regulation of biofouling and sinking of MPs.

1. Introduction

Plastic pollution is a growing global concern that has attracted interest from the public, policymakers and scientists (Rochman and Hoellein, 2020). Numerous studies have been performed to identify and quantify the sources, transport and fate of plastic waste within the atmosphere, terrestrial, and freshwater/marine environments (Cózar et al., 2014; Jambeck et al., 2015). Once plastic items are discarded into the environment, they fragment into smaller particles due to photooxidation, physical erosion and biodegradation (Andrady, 2017). Consequently, the small plastic particles within the size range of 1 μm–5 mm defined as microplastics (MPs), are numerically much more abundant than larger plastic debris in the environment. Notably, the global estimation of MPs suspended in the ocean is only ~1% of annual global plastic inputs to the ocean (Koelmans et al., 2017). This overwhelming discrepancy between the amount of MPs supposedly exported by rivers to the ocean and the MP stocks accumulating at the ocean surface has triggered the idea of a "missing" ocean plastic sink (Thompson et al., 2004; Cózar et al., 2014).

Although there remains considerable controversy concerning the missing oceanic sink (Weiss et al., 2021), a large amount of plastics have been recovered from seafloor sediments (Kane et al., 2020), which infers the deep ocean is an ultimate sink for plastics (Woodall et al., 2014; Cózar et al., 2017). Freshwater sediment has also been considered as a transient or terminal sink for MPs (Leiser et al., 2021; Yang et al., 2021). Several hypotheses are proposed to explain the removal of MPs from surface waters (Michels et al., 2018; Foekema et al., 2013; Cole et al., 2016; Reisser et al., 2015; El Hadri et al., 2020), whereas the sinking of MPs caused by a density increase after biofouling (i.e., rapidly colonization of submerged MP surfaces by microorganisms) is considered to be an important pathway for the downward transport of MPs in the ocean and freshwaters (Fazey and Ryan, 2016; Kooi et al., 2017; Kaiser et al., 2017; Amaral-Zettler et al., 2021; Semcesen and Wells, 2021). The sinking versus floating of MPs due to biofouling not only affects the

* Corresponding author.
E-mail address: xshang@wmu.edu.cn (X. Shang).
[1] These authors contributed equally to this work.

https://doi.org/10.1016/j.watres.2022.118656
Received 26 January 2022; Received in revised form 28 April 2022; Accepted 23 May 2022
Available online 24 May 2022

vertical distribution of MPs in the water body, but also their horizontal distribution (Ryan, 2015; Kooi et al., 2017). Therefore, quantifying the sinking dynamics of MPs after biofouling is vital for understanding the vertical and horizontal diffusion of MPs in different water bodies, which is further essential for simulating and estimating the global distribution and final fate of MPs in aquatic systems.

While plastic debris with densities greater than water will tend to sink and be incorporated in sediments, plastics less dense than water are expected to float and may eventually pass through open aquatic systems of lakes and rivers, ultimately ending up in the ocean (Ballent et al., 2016). However, microbial growth (biofilm) on the surface of low density MPs can lead to an overall density increase and hence cause sinking (Fazey and Ryan, 2016; Semcesen and Wells, 2021). Moreover, the development of complex microbial biofilms facilitates the adhesion of suspended dense materials like marine snow and iron hydroxides, which further enhances the overall density and speeds the sinking of MPs (Michels et al., 2018; Leiser et al., 2020). Both model simulations (Kooi et al., 2017) and *in situ* experiments (Fazey and Ryan, 2016; Chen et al., 2019) have investigated how biofouling alters the buoyancy of MPs in both marine and fresh waters, and the size-specific sinking rates caused by biofouling may be one reason for the apparent paucity of small MPs floating in the surface ocean (Ryan, 2015). Kooi et al. (2017) posited that biofouling-induced increases in density result in small MPs entering the deep ocean, whereas large MPs have a higher chance of remaining at the ocean surface. However, Rummel et al. (2017) suggested that MPs with a size of about 5μm tend to sink more easily, while smaller and larger MPs tend to float. The discrepancy among these results highlights the complexity associated with the sinking behavior of MPs due to biofouling.

Most of the existing *in situ* and *ex situ* experimental results tend to support that small MPs with higher surface area to volume ratios (SA:V) are more likely to sink after biofouling (Fazey and Ryan, 2016; Chen et al., 2019; Semcesen and Wells, 2021). However, MPs of the same volume but different shapes have different SA:V ratios, which complicates the sinking of MPs due to biofouling. Larger plastic films with lower SA:V ratios than smaller films may sink more easily, implying that other factors, such as shape creates drag force variations affecting the sinking behavior of MPs (Van Melkebeke et al., 2020; Amaral-Zettler et al., 2021). The judgement of floating/sinking status of incubated MPs in these studies was indirectly estimated according to the overall density change of plastic particles immersed below the water surface. Furthermore, the buoyancy difference of MPs with different sizes and shapes was indirectly determined from the sinking probability or sinking velocity calculated according to the change in density (Fazey and Ryan, 2016; Kaiser et al., 2017). There are several shortcomings in these indirect measurements based on the overall density change. First, the difference in biofilm development between floating and suspended MPs is ignored (such as not all surfaces are colonized equally, defouling may occur due to abrasion from water mixing, etc.); this is especially important for comparing the sinking behavior of MPs with different original densities; Second, the indirect method for estimating the initiation of sinking will be highly variable whether it is based on faster biofilm growth of immersed versus the slower biofilm growth of floating MPs; Third, the sinking behavior of smaller MPs is complicated by aggregation dynamics and adherence to experimental devices rendering conclusions concerning the sinking rates of smaller plastic particles extrapolated from macro- and mesoplastic experiments unreliable (Fazey and Ryan, 2016). Recent *ex-situ* evidence demonstrated faster sinking of smaller plastic particles (Semcesen and Wells, 2021), however, this size-specific sinking relationship requires further *in situ* verification. Therefore, although determining the sinking rates of small plastic items drifting in open water is a crucial step for understanding global MP dynamics, existing experimental and modeling approaches still encounter several logistical challenges.

In order to visually document the sinking dynamics of initial free floating MPs due to biofouling, we developed an *in situ* incubation and monitoring experiment to simulate natural biofilm development in a eutrophic river. We assessed the sinking behavior of MPs after biofouling as a function of polymer type (polyethylene (PE), polypropylene (PP), and expanded polystyrene (EPS)), particle shape (granule, fiber, film) and granule size (~ 0.06, 0.36, and 1.95 mm equivalent spherical diameter for small, medium, and large granules, respectively). Although the densities of the studied polymers ($\leq$ 0.96 mg/mm^3) were all lower than fresh/ocean waters, PE and PP MPs are commonly found in aquatic sediments. Notably, the density of foamed plastics, such as EPS (0.02 mg/mm^3), is much lower than water, but they are prevalent in freshwater (Vaughan et al., 2017) and marine sediments (Sagawa et al., 2018), with biofouling speculated as the primary reason for their sinking. By tracking the biofouling process of MPs introduced as floating particles rather than as immersed particles in previous research, this study attempts to provides a better simulation of how real-world MPs, including EPS whose density is much lower than that of water, are impacted by biofouling to alter their floating/sinking dynamics in aquatic systems. Moreover, the paradigm of whether smaller particles sinking faster is applicable for MPs smaller than 100 μm was tested, and how the SA:V ratio related to different particle shapes affects the sinking behavior of MPs was further assessed.

2. Materials and methods

2.1. Properties of experimental MPs

Experimental MPs were purchased from various manufacturers, including granules of 3 common polymer types, PE (0.95 mg/mm^3), PP, (0.91 mg/mm^3) and EPS (0.02 mg/mm^3), and fibers and films of PE. We used 3 sizes (small: ~ 0.0008 mm^3 volume, medium: ~ 0.19 mm^3 volume, large: ~ 31 mm^3 volume) of granules for each polymer type, and the original PE fibers (~ 0.22 mm diameter) and films (~ 0.05 mm thickness) were cut into size-volume dimensions having a mass similar to the medium-size granules (Fig. S1). Overall, this designed resulted in 11 different experimental MPs: 3 granular polymer types × 3 sizes + PE fibers + PE films. Detailed properties of the experimental MPs (Table S1) and density measurements can be found in protocol 1 in Supplementary Materials.

2.2. In situ incubation, observation and sampling

The *in situ* incubation was conducted in a branch of the Wen-Rui Tang River, a typical low-gradient urban river located on the coastal plain in Wenzhou, Zhejiang Province, southeast China. This area is one of the most rapidly developing regions in China. Rapid urbanization and industrialization often overburden the sewage treatment system resulting in eutrophication of river waters (Mei et al., 2014). Our previous studies documented massive deposition of MPs in riverine sediments in this area (Wang et al., 2018; Yao et al., 2019; Ji et al., 2021).

Since MPs cannot be tracked and observed if they are directly dispersed on the water surface, we designed incubators built from drinking water bottles. Incubators were deployed *in situ* to allow for natural biofilm development under ambient environmental conditions and to facilitate observation and sampling to track the sinking of biofouled MPs (Fig. 1a). The drinking water bottle (PET body and HDPE cap) was cut off about 1/3 of the length from the bottle mouth, and the upper and lower parts bonded back together with adhesive tape. Cuts on the cap (6 pores of ~ 1 mm diameter) and body (2 openings of ~ 3 mm maximum width) of the incubators enabled the free exchange of air, water, plankton and fine suspended materials in and out of the bottle during incubation. However, the relatively small cuts prevented the loss of MPs during incubation. The incubators were fixed on foam floatation beds to maintain a constant depth with respect to the water surface (Fig. 1b). The consistent air, water and air-water interface conditions inside and outside the incubator make the simulation of biofouling and subsequent sinking of MPs realistic with respect to real-world

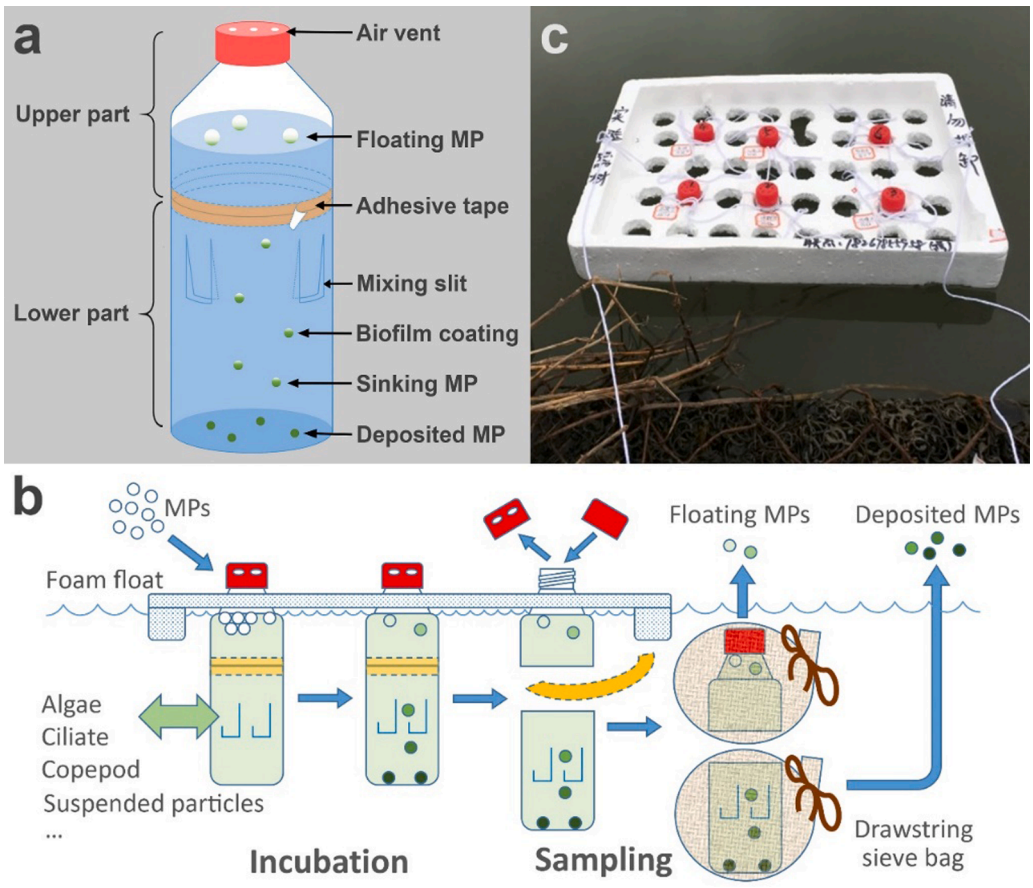

Fig. 1. Diagram of incubation bottle (a), incubation and sampling processing (b), and a photo following deployment of the *in situ* incubation system in river (c).

environmental conditions (Fig. 1c).

Once the floatation beds were deployed on the water surface ~0.5 m offshore, MPs of specific size, shape and polymer type were applied to the water surface of each incubator and then inserted into the floatation platform. The number of large MPs in each incubator was 20, and the number of medium and small MPs in each incubator was 50. In order to track the development of biofilms on the MPs, triplicate incubators were randomly collected from each experimental group (same size, shape and polymer type) every 6 days during the 30-day experiment for a total of 5 sampling times. There were 15 replicates at the beginning for each specific treatment group and 11 specific treatment groups for a total of 165 incubation chambers (Table S2). The tracking of the floating/sinking status of biofouled MPs utilized two strategies according to the observation convenience/effectiveness corresponding to MP particle size. The large and medium floating MPs were counted based on a photo of the whole water surface inside the incubator, which was taken by camera after removing the bottle cap of all remaining incubators every 3 days. Because small MPs remaining on the water surface were not distinguishable in a photograph, their floating/sinking status was tracked by enumerating the floating and sinking particles recovered from the 3 incubation chambers collected every 6 days for biofilm measurement.

Sampling of incubated MPs for biofilm analysis was started by replacing the vented cap with a non-vented cap, to ensure that no MPs escaped from the vented cap during sampling. Then, the incubator was gently removed from the floating bed, and after removing the adhesive tape between the upper and lower parts under the immersed state, both chambers were quickly placed into sieve bags with a 38 μm aperture (Fig. 1). The MPs recovered from the upper and lower chambers of the incubator were regarded as "floating" and "sinking" MPs, respectively. Any MPs adhering to biofilms on the incubator wall were considered as sinking MPs. The consistency of the two counting strategies was verified by comparing the floating/sinking results of large and medium MPs derived from both methods.

2.3. Sample analysis

Water quality at the incubation site was monitored every 6 days during the incubation period at the time of MP sample collection. The temperature, pH, dissolved oxygen (DO), chlorophyll-a and turbidity were measured *in situ* by a multiparameter probe (YSI-EXO2, Xylem, USA) in the afternoon of each sampling date. A one-liter water sample was taken for analysis of ammonia nitrogen (NH_4^+-N), nitrate nitrogen (NO_3^--N), nitrite nitrogen (NO_2^--N), phosphates (PO_4^{3-}-P), total nitrogen (TN), total phosphorus (TP).

The composite density (i.e., combined density of MPs + biofilms) after biofouling is the key parameter affecting the floating/sinking status of MPs. However, it is difficult to measure the composite density or the biofilm mass of each individual MP. Measurement of just a few individual MPs is also unreliable as the overall biofilm development can be highly heterogeneous on different MPs. Therefore, we use the total biomass of biofilms on all MPs in each incubator to characterize the overall growth of biofilms at each stage, and used this as the basis to calculate the composite density of biofouled MPs. Detailed biofilm mass measurements can be found in protocol 2 in Supplementary Materials.

Once the composite density of the biofouled MPs exceeds the ambient water density, the sinking of MPs is expected. The composite density of the biofouled MPs was calculated using Eq. (1). Where D_{com} is the composite density of the biofouled MPs; M_{mp} is the mass of original MPs; M_{bf} is the dry mass of biofilm; V_{mp} is the volume of original MPs; and V_{bf} is the volume of biofilm.

$$D_{com} = \left(M_{mp} + M_{bf}\right) / \left(V_{mp} + V_{bf}\right) \quad (1)$$

The volume of biofilm (V_{bf}) was calculated using Eq. (2). Where ρ_{bf} is the density of biofilms. Since the biofilm density used in previous studies ranges from 1.1 to 1.5 mg/mm^3 (Lagarde et al., 2016; Kooi et al., 2017; Van Melkebeke et al., 2020; Amaral-Zettler et al., 2021), we set ρ_{bf} at 1.25 mg/mm^3, which is close to the value measured from diatom biofilms (Amaral-Zettler et al., 2021) and the empirical value used in other studies (Kooi et al., 2017; Van Melkebeke et al., 2020).

$$V_{bf} = M_{bf} / \rho_{bf} \quad (2)$$

By comparing the composite density (D_{com}) of MPs derived from Eq. (1) and the density of freshwater (1.0 mg/mm^3), the general possibility of biofouled MP sinking can be assessed.

2.4. Statistical analyses

The floating/sinking MPs and biofilm data were analyzed by SPSS 20.0 (IBM, Armonk, NY, USA). Normality of the data was tested using the Shapiro-Wilk's test and log transformation were used as necessary to assure that the residuals were normally distributed. Variation in the amount of floating/sinking MPs, biofilm mass, and the composite density of biofouled MPs among treatments were assessed using one-way ANOVA, followed by the Holm-Sidak all-pairwise multiple comparison test. All data are reported as mean ± SD, unless otherwise stated. All "differences" referred to in presentation of the results denote a statistical significant at least of $P < 0.05$.

3. Results

3.1. Environmental parameters

During the experimental period, the quality of the surface water around the incubators showed some degree of variability, but no discernable trends (Table S3). The afternoon temperature of the surface water was 23.3 ± 0.9 ℃. Nitrate (1.96 ± 0.29 mg/L) was the main form of nitrogen followed by ammonium (0.47 ± 0.13 mg/L) and low levels of nitrite and organic N; phosphate (0.10 ± 0.05 mg/L) was the dominant form of TP (0.15 ± 0.05 mg/L). Favorable temperature and abundant inorganic N/P concentrations yielded relatively high Chl-a concentrations (23.9 ± 10.3 μg/L). A correspondingly high DO (7.76 ± 1.53 mg/L) reflects active DO production from algal photosynthesis. A moderate turbidity of 12.7 ± 1.7 NTU implies relatively good light conditions to promote algae biofilm growth in surface water.

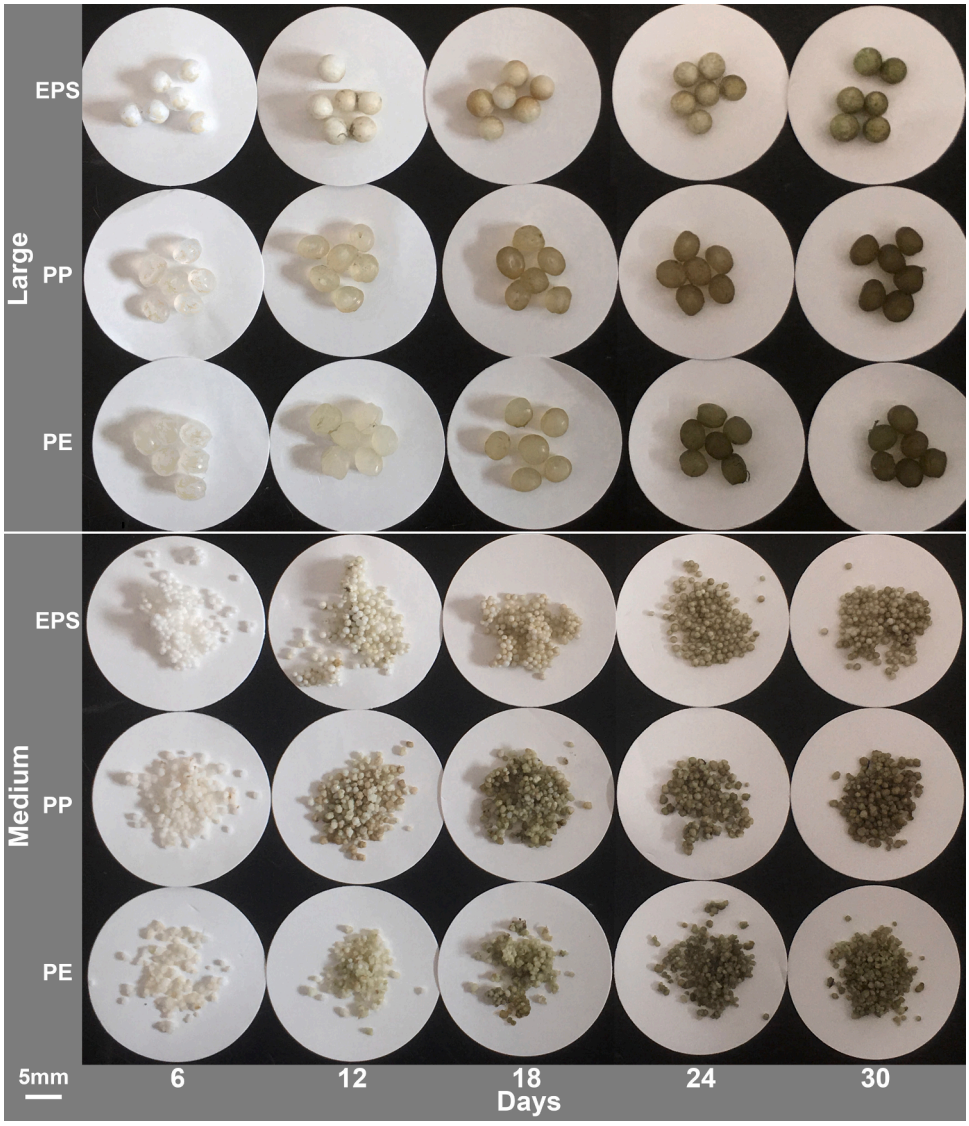

Fig. 2. Biofilm development on the large (~31 mm^3) and medium (~0.19 mm^3) MP granules during the 30-day incubation.

3.2. Development of biofilms on MPs

Biofilm was visibly developed on the surface of incubated MPs, and the coverage by biofilms progressively increased with time (Fig. 2). While not specifically quantified, visual observation via a light microscope revealed that the biofilms were dominated by algal cells with minimal inorganic materials; however, fine inorganic particles (e.g., silt, clay) maybe obscured by algal cells. In the early incubation stage, there was no significant difference in biofilm development on MPs of different polymer types, sizes or shapes. As the incubation progressed, variations in biofilm mass became increasingly more evident on the contrasting MP substrates (Figs. S2 and S3).

Biofilm mass per unit MP mass of medium and large EPS granules was significantly higher than that of PE and PP granules after 24 days of incubation ($P < 0.05$) (Fig. S2A). This does not imply that biofilm development on EPS granules was faster, but rather was due to the much lower density of the original EPS material. In fact, the biofilm mass per unit volume of EPS granules was significantly lower than that of PE and PP granules beginning on the 12th day for medium MPs, and 24th day for large MPs ($P < 0.01$) (Fig. S2B). The biofilm mass per unit surface area of EPS granules was only ~ 1/20 of that of PE and PP granules at the end of the 30-d experiment (Fig. S2C).

The biofilm mass per unit mass/volume of medium PE and PP granules were both significantly higher than that of the large MPs beginning on day 12 ($P < 0.05$), whereas these two indexes for medium EPS granules were higher than that of large EPS granules from day 24 ($P < 0.05$) (Fig. S2A and B). There was no variation in biofilm mass per unit surface area between medium and large MP granules at most sampling times, except for medium PP granules being higher than large PP granules at day 18 ($P < 0.05$) (Fig. S2C). This indicates that the thickness of biofilms growing on MPs of the same polymer type within a given time period was similar, regardless of its size.

The variation of shape-specific biofilm development was not as significant as the size-specific variation. Biofilm mass per unit mass/volume did not vary among medium PE MPs of granule, fiber or film shapes at most sampling times, except for the biofilm mass per unit mass of PE films that increased faster and was higher than that of granules at the end of experiment ($P < 0.05$) (Fig. S3A and B). Notably, the biofilm mass per unit surface area of medium PE films from day 18 and fibers at day 30 was significantly lower than that of medium granules ($P < 0.05$). The biofilm mass per unit surface area of medium PE films was also significantly lower than that of fibers at day 18 and 24, but no significant variation between these two shapes was measured at day 30 (Fig. S3C).

3.3. Sinking dynamics of MPs

More than 99% of the MPs were recovered from the experimental chambers following field incubation and sample processing. In general, the total amount of floating MPs counted by physical sampling of the upper and lower compartments of the incubator chambers (3491) was slightly higher than that counted from photographs (3429) for large and medium MPs. Hence, a strong linear correlation ($R^2 = 0.99$) was obtained between the two categories of data collection documenting that the floating/sinking status of MPs derived from these two enumeration methods yielded the same results (Fig. S4). Therefore, the floating/sinking tendency of small MPs derived exclusively from the physical sampling method was deemed comparable with respect to the data for the large and medium MPs.

The onset time for MP sinking varied among biofouled granules of the same size but different polymer types (Fig. 3). For large MP granules, only the PE MPs were observed to sink beginning on the 24th day; whereas no large PP or EPS granules sank during the 30-d incubation. Overall, the variation in floating/sinking status was not significant among large MPs of different polymer types (Fig. 3A). The observed onset times for sinking of medium PE and PP granules were the 15th and 12th days, respectively, with no significant variations in floating/sinking proportions noted between the two polymer types. The majority of PE and PP medium granules sank by the end of the experimental period, whereas all medium EPS granules remained floating (Fig. 3B). Small MPs of all three polymer types sank much sooner than their larger counterparts during the incubation period. The onset of sinking for small PE and PP granules was earlier than the first observation time on day 6 when sinking particles represented 49 ± 11% for PE and 28 ± 15% for PP. The sinking of small EPS granules was first observed on day 12, which was noticeably delayed compared to the PE and PP polymer types

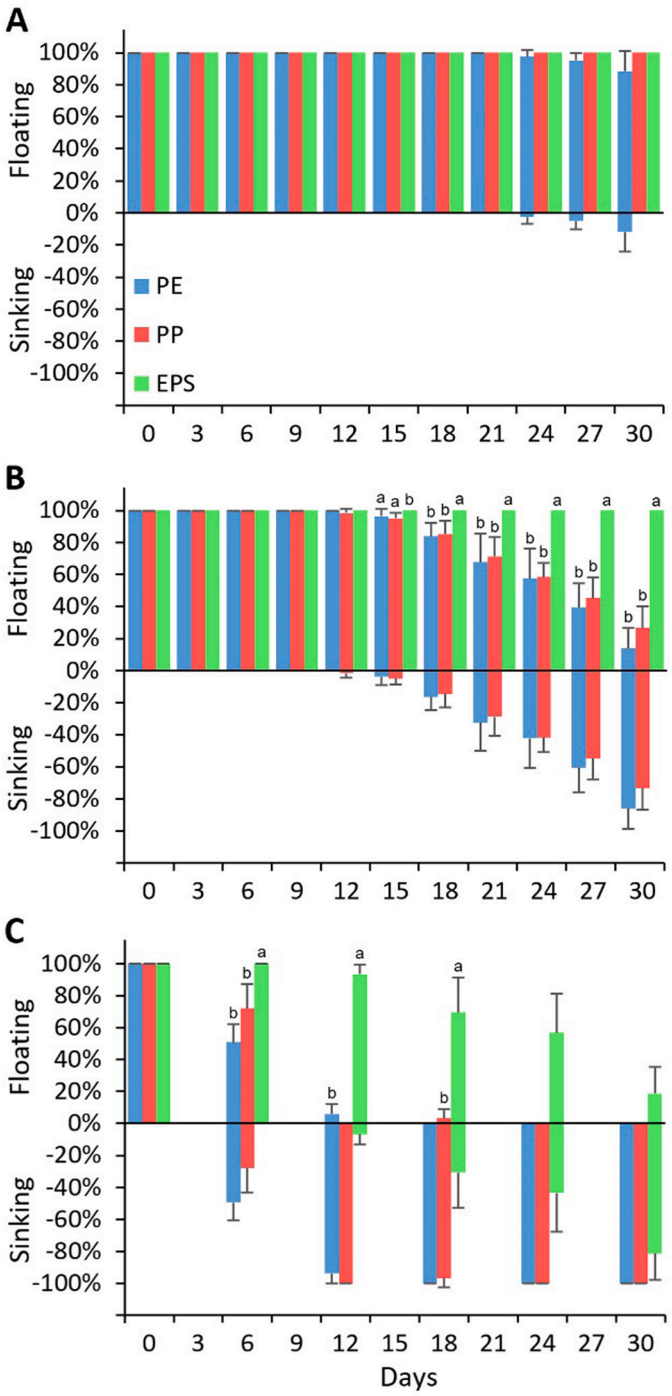

Fig. 3. Polymer-specific floating/sinking status (mean ± SD) for MPs of different size groups during incubation. A: Large (~ 31 mm^3); B: Medium (~ 0.19 mm^3); C: Small (~ 0.0008 mm^3). Statistical differences between the 3 polymer types at a given time are indicated by different lower case letters ($P < 0.05$).

(Fig. 3C).

For granules of the same polymer type, the smaller MPs sank earlier than the larger ones. Nearly all of the small PE and PP MPs disappeared from water surface after 12 days of incubation, whereas almost no medium and large PE and PP MPs began sinking before then. Once sinking of PE and PP medium granules began after 15 days of incubation, the amount of floating particles decreased over time. Only 14 ± 12% of PE and 27 ± 13% of PP medium granules remained floating until the end of experiment, whereas 88 ± 13% of PE and 100% of PP large granules remained after 30 days (Fig. 4A and B). No sinking was observed for medium and large EPS granules, whereas small EPS granules began sinking on day 12 and only 19 ± 17% remained floating at the end of the 30-d incubation (Fig. 4C).

The sinking behavior for MPs of the same polymer type and volume, but different shape, hence a different SA:V ratio, was anticipated to be appreciably different. Unexpectedly, the variation of floating/sinking proportions among the medium-size PE MPs of granule, fiber and film shapes was not evident at most observation times (Fig. 4D). Although the PE fibers with a higher SA:V (Table S1) than PE granules sank slightly earlier, the PE films with an even higher SA:V began to sink at the same time as the granules. The sinking proportion of fibers was higher than granules at days 15 and 18 ($P < 0.05$), but was not significantly different at subsequent observation times. While having similar onset times for sinking, the sinking proportion of films occurred at a higher rate than that of granules at day 24 ($P < 0.05$). However, there was no variation among the sinking proportions of the three different MP shapes at the end of the experimental period.

3.4. Effects of biofilms on the buoyancy of MPs

The increase of composite density for MPs after biofouling led to their loss of buoyancy. Because small MPs were engulfed and aggregated by large biofilms making them difficult to separate, only the composite density of large and medium MPs were estimated after biofouling. The temporal composite density pattern for biofouled MPs was similar to that of the accumulated biofilm mass. The composite density for all MPs progressively increased with the development of biofilms throughout the incubation. However, given the differences in the density of the original polymer types, the floating/sinking status alteration caused by the changes in the composite density was different among the polymer types (Fig. 5).

The composite density of the biofouled medium and large EPS granules was always far lower than the water density, which was consistent with the phenomenon that no medium or large EPS MPs sank during the incubation period (Fig. 5A). The composite density of PE granules was significantly higher than that of PP granules at the beginning of the incubation period, and the composite density difference between the large granules of these two polymer types remained throughout the incubation period. In contrast, differences in the composite density between the medium PE and PP granules were no longer significant after day 18 (Fig. 5A). Notably, the composite density of large PE and PP granules was lower than water density throughout the incubation, whereas the average composite density of medium granules was higher than the water density after day 24 for PE and after day 30 for PP.

The trend in composite density of PE MPs with different shapes during the early biofouling period was similar. Differences in the SA:V among the three shapes did not affect the growth of biofilms and composite density at this early stage. However, the composite density of fibers and films increased during the later stages of the incubation when compared to granules. The composite density for all three MP shapes exceeded that of water at day 24, with the composite density of films being significantly higher than granules after day 24 (Fig. 5B).

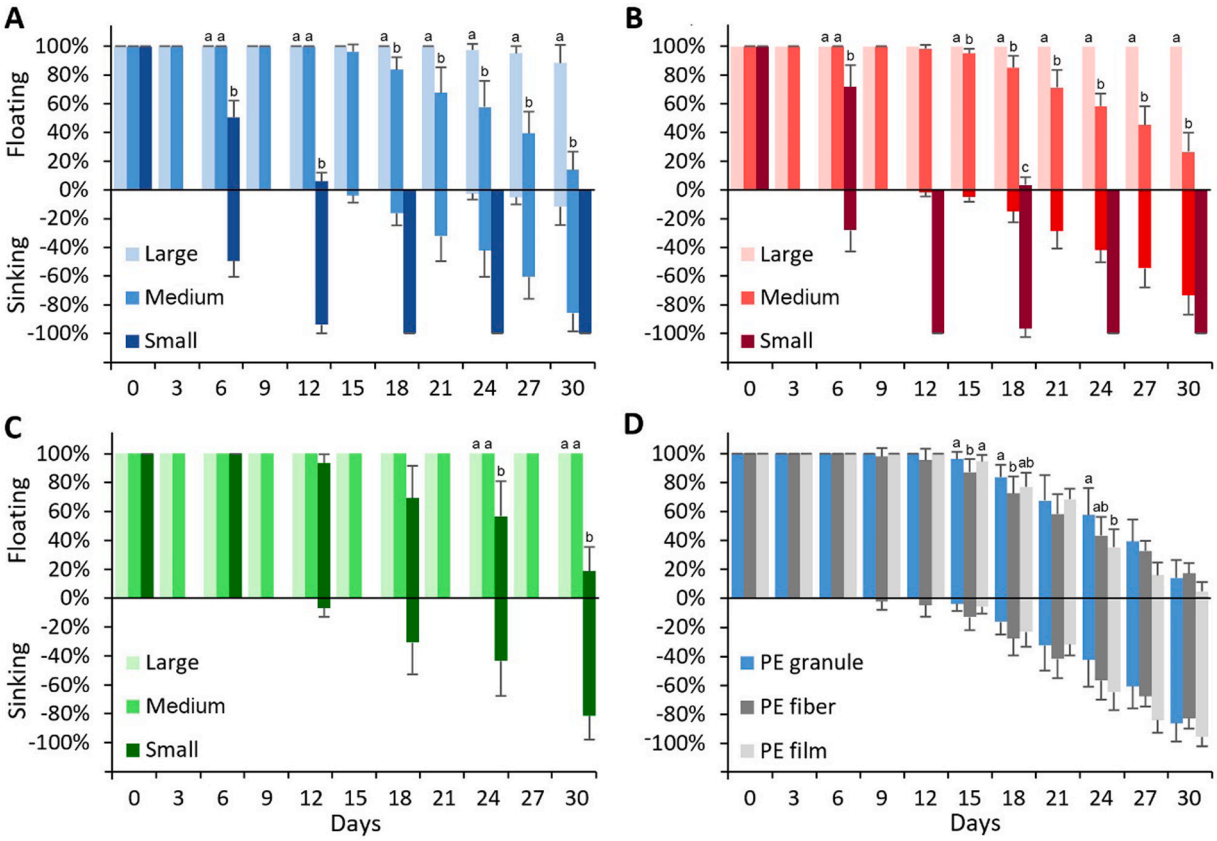

Fig. 4. Size-specific floating/sinking status (mean ± SD) of MPs of different polymer types, sizes and shapes during the 30-d incubation period. A: PE granules; B: PP granules; C: EPS granules; D: Medium size PE MPs. Significant differences ($P < 0.05$) in the proportion of floating versus sinking particles for the three sizes/shapes at a given sampling time are designated with different lower case letters.

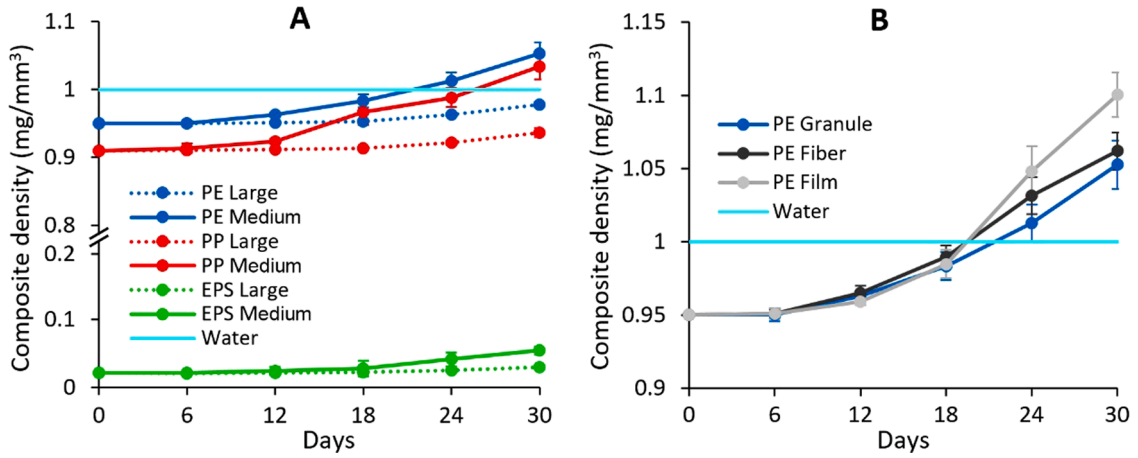

Fig. 5. Composite density (mean ± SD) change of biofouled MPs during the 30-d incubation. A: Size-specific variation of MPs of different polymer types; B: Shape-specific variation of PE MPs.

4. Discussion

4.1. Biofilm development on MPs

Biofouling is considered a key factor regulating the floating versus sinking of MPs, especially for those MPs with low densities (Kaiser et al., 2017). Once released into aquatic environments, a biofilm coating consisting of inorganic and organic substances, is progressively formed on MPs beginning within minutes to hours (Cooksey and Wigglesworth-Cooksey, 1995; Lobelle and Cunliffe, 2011; Oberbeckmann and Labrenz, 2020). Our study showed that the growth of biofilms was slow during the initial stages of MP incubation, but biofilm growth was exponentially once the biofilms became established on all the MPs of different polymer types, sizes and shapes. With the increase in composite density above that of ambient water (1.025 mg/mm^3 for surface sea water and 1.000 mg/mm^3 for fresh water at 25 °C), the sinking of MPs becomes inevitable (Long et al., 2015). This effect is likely to be further intensified by the aggregation of biofouled MPs (Michels et al., 2018), such as for the small MPs encountered in this study.

Most existing studies examining biofilm growth on plastic surfaces involved incubation by fully immersing the plastics in the water column (Fazey and Ryan, 2016; Kaiser et al., 2017; Chen et al., 2019; Tu et al., 2020; Miao et al., 2021). However, this immersion incubation approach is more reflective of biofouling conditions after "sinking" rather than biofouling associated with the initially "floating" particles. Based on the growth characteristics of biofilms on EPS MPs in this study, large variations may exist between surface versus immersion biofouling processes. Previous studies inferred that the biomass of biofilms grown on EPS MPs will be similar to PE and PP MPs per unit volume when they are all incubated underwater (Tu et al., 2021). However, we found that the biofilm biomass per unit volume or surface area on EPS MPs was much less than that on PE and PP. This implies that the preferential immersion of denser MPs accentuates biofilm growth owing to greater growth under immersed conditions as compared to floating conditions. Under the natural floating state, only a small volume of the EPS surface is submerged in water and available for biofilm growth, about 1/12 at the beginning of the incubation and gradually increasing as biofilm growth and density increase. As a result, the substrate area for biofouling prior to immersion is much smaller for less dense EPS MPs, resulting in lower total biofilm mass. Therefore, more “natural” incubation conditions incorporating both the floating and immersion phases are required to effectively simulate the biofouling process encountered by floating MPs.

Biofilm development on the surface of MPs is often characterized by surface coverage (Fazey and Ryan, 2016), cell abundance (Tu et al., 2020), weight (mass of biofilm or composite mass of biofilms + MPs) (Kaiser et al., 2017; Miao et al., 2021) or biomass per unit surface area/volume (Chen et al., 2019). Given all the different biofilm metrics among published studies, it is hard to make direct comparisons of MP biofilm development between different studies. Because the initial density, size and shape of MPs varied in this study, there were significant variations in reporting biofilm mass in unit of substrate mass, volume and surface area. Interconversion among these quantitative units implies an assumption of uniform biofilm coverage and density, further complicating the reporting and comparison of MP biofouling among studies.

The growth of biofilms on MP surfaces is regulated by many environmental factors, including temperature, water flow, nutrients, turbidity and composition of biological and abiotic suspended materials. Therefore, the growth rate of biofilms is likely to be appreciably different in contrasting water bodies (Miao et al., 2021), different depths within the water column (i.e., light limitation, Smith et al., 2021) and different seasons (Chen et al., 2019). Biofilms can grow at astonishing rates on the surface of submerged items under favorable environmental conditions. Microbes were shown to colonize MP surfaces in offshore environments within a few hours, and biofilm formation reached a steady-state within 14 days (Harrison et al., 2014). The thickness of fouling coatings can reach 1 mm within one week in bioreactors (Murga et al., 1995), and up to several centimeters on the surface of plastic blocks after 10 weeks of offshore incubation (Fazey and Ryan, 2016). The warm water temperature, favorable nutrient concentrations, moderate turbidity and low water flow associated with the incubation environment in our study were deemed highly favorable for the growth of biofilm. Once the biofilms were established, the growth rate became exponential after an initial period of slow colonization. In addition to environmental factors, the development of biofilm on plastics is believed to depend on polymer type, specific surface area, surface energy and roughness (Ye and Andrady, 1991; Kerr et al., 2003; Andrady, 2011; (Artham et al., 2009)), thereby causing significant variation in the floating/sinking behaviors of different MPs due to biofouling.

4.2. Effect of polymer type on MP floating/sinking dynamics

Differences in the growth of biofilms on the different polymer types resulted in different floating/sinking behavior of the biofouled MPs. Although a few large PE granules sank while no large PP granules sank during the incubation, there was no significant variation in the sinking behavior between PE and PP granules after biofouling. This finding was attributed to the similar initial density of the PE (0.95 mg/mm^3) and PP (0.91 mg/mm^3) polymers. As the most common polymers in marine and freshwater environments, the density of PE and PP is less than that of both fresh and marine waters, hence they should naturally float on the water surface. However, both PE (Fazey and Ryan, 2016; Amaral-Zettler

et al., 2021) and PP (Chen et al., 2019; Semcesen and Wells, 2021) MPs can eventually sink as their composite density increased due to the growth of biofilms on their surface. Nevertheless, one study employing an immersion incubation showed that the composite density of PP MPs actually decreased after biofouling, whereas the composite density of biofouled PET increased using the same incubation conditions (Miao et al., 2021). This suggests that the biomass and community structures of biofilm grown on MPs might differ among polymer types (Nava et al., 2021), which has been attributed to the morphology/surface texture rather than polymer composition (Parrish and Fahrenfeld, 2019). Other studies found that the biofilm mass grown on EPS was higher than PE and PP using a submerged incubation (Tu et al., 2021), which differed with our findings of much lower biofilm mass on natural floating EPS MPs compared to PE and PP MPs.

EPS is the foamed form of polystyrene (PS) that contain a high proportion (> 95%) of air-filled porosity making its density much lower than other common plastics (Turner, 2020). The first impression of EPS being too light to sink conflicts with real-world observations of sinking EPS MPs. As an prevalent components of plastic litter in aquatic environments, EPS MPs are commonly found in both marine and freshwater sediments (Vaughan et al., 2017; Sagawa et al., 2018). Thus, there must be some mechanism that causes EPS MPs to sink, and the loss of buoyancy due to biofouling is a prevailing theory. In our study, the large- and medium-sized EPS granules did not sink; however, the small EPS MPs did sink, albeit at much lower rate than their PE and PP counterparts. Field observations also provide evidence that the sinking of EPS MPs was associated with the particles being trapped and sinking with large biofilms. Furthermore, EPS is more likely to weather into smaller particles via exposure to UV radiation and mechanical fragmentation than other common plastics (Efimova et al., 2018). Thus, the sinking of small EPS MPs after biofouling might be an important mechanism controlling the fate of the massive EPS debris pool in the global environment.

4.3. Size-specific floating/sinking dynamics of MPs

Biofouling has been posited as a size-selective mechanism in shaping the composition of floating plastic debris (Ryan, 2015). For example, there is an overwhelming dominance of small size fractions among MPs accumulated in sediment, implying a higher sinking tendency for small MPs (Wang et al., 2018; Mani et al., 2019; Kane et al., 2020). While small plastic items near the upper size limit of MPs (5 mm) have been demonstrated to sink faster than larger fragments, it has not been established whether this rule can be extrapolated to the full range of MP size classes (Fazey and Ryan, 2016). Although information regarding size-specific sinking of MPs under immersed incubation conditions is recently increasing (Fazey and Ryan, 2016; Kaiser et al., 2017; Chen et al., 2019), reports concerning the sinking of free-floating MPs after biofouling, especially small MPs, is still scarce (Semcesen and Wells, 2021). Wright et al. (2020) determined that a biofilm with a 10-μm thickness was sufficient to cause PE spheres < 100 μm to sink. Moreover, our results demonstrated that the paradigm of smaller MPs sinking faster was valid for MPs down to a size of at least 100 μm. Since particles as small as 5–50 μm could have sufficient surface area and roughness to allow colonization of bacteria (generally 0.5–1.5 μm long; Kerr et al., 2003), it may be expected that the concept of smaller MPs sinking faster after biofouling will be applicable for MPs smaller than 100 μm as well.

In our study, nearly 50% of PE and 30% of PP small granules sank after 6 days of incubation. As a comparison metric, we calculated the time required for the sinking of 50% of the MPs from the relationship between incubation time and the sinking fraction. The 50% sinking time ratio for PE, PP and EPS small granules was 6.1, 7.7 and 23.8 days, respectively. Similar sinking times for PE and PP medium granules were 24.4 and 25.4 days. Our 50% sinking rate versus size relationship was similar to that reported by Fazey and Ryan (2016), but differed from Semcesen and Wells (2021) (Fig. 6). If the logarithmic relationship between MP size and sinking time is also applicable to smaller MPs, it can

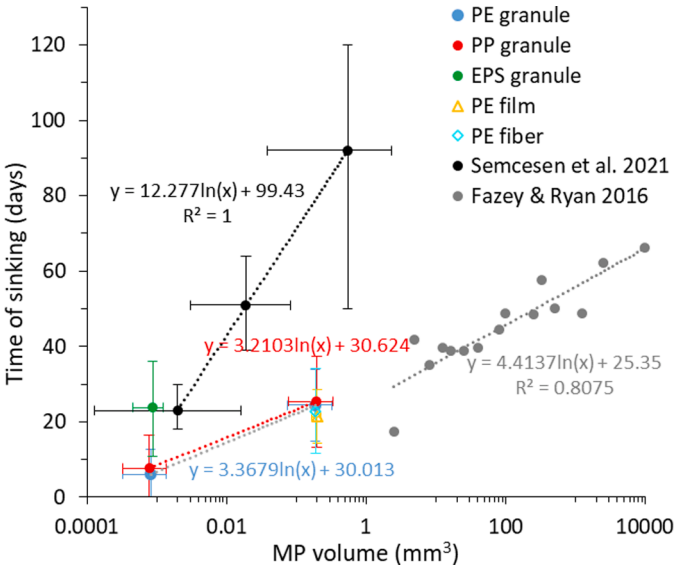

Fig. 6. Comparison of studies reporting the relationship between the time required for sinking of 50% of MPs (small and medium size) and MP sizes. Whiskers represent the minimum and maximum values for sinking time and volume of plastic particles.

be estimated that after 1 day of incubation, half of the PE MPs smaller than 197 μm, 85 μm and 70 μm would sink in the coastal ocean (Cape Town, South Africa), Simcoe Lake (southern Ontario, Canada) and the eutrophic river in this study, respectively. Because the biofilm growth on MP surfaces is slow at the initial stage of microbial colonization, the actual sinking time of MPs maybe longer than these estimates. The rapid sinking of MPs after biofouling might play a substantially role in decreasing riverine input and increasing deep-sea output, thus provides a potential mechanism for addressing the "missing" plastic debate at the ocean surface.

4.4. Shape-specific floating/sinking dynamics of MPs

Shape is also considered as an important factor affecting the sinking of biofouled MPs (van Melkebeke et al., 2020; Amaral-Zettler et al., 2021). In particular, the SA:V is often used to interpret the variation of biofilm growth and sinking of MPs with different shapes (Ryan, 2015; Amaral-Zettler et al., 2021; Semcesen and Wells, 2021). However, PE fibers and films with higher SA:V than granules of similar mass did not sink faster in this study. Field observation showed that biofilm growth was much slower on the upper versus bottom side of the floating films, hence only half of the surface area was fully colonized by microbes. This differential growth dynamic appears to explain the late sinking onset for the floating MP films in our study compared to previous studies employing immersed incubation. As the initially floating MP films became progressively more submerged due to sinking in the later stage of the incubation, the overall biofilm mass on the MP films increased rapidly and eventually exceeded that of the granule particles.

Further, the impact of the drag coefficient determined by the shape of the particle cannot be ignored in assessing the floating/sinking behavior of MPs during biofouling. Hydrodynamic drag is an important parameter affecting the sinking behavior of particles moving through a fluid (Crowe, 2005). Hence, variations in the drag coefficient induced by particle shape will significantly affect the sinking speed of particles, such as demonstrated for algae (Padisák et al., 2003). The drag coefficient of film or fiber particles is significantly higher than that of granules, thereby possibly offsetting to some extent the sinking potential caused by the buoyancy loss of biofouled MPs. The similar sinking behavior among MPs with the same mass but large SA:V differences in this study suggest shape factors other than SA:V may also contribute to sinking

dynamics. Moreover, observations that "macroplastic" films having very high SA:V sink faster than "microplastic" fragments (Amaral-Zettler et al., 2021) implies that the impact of particle shape on the floating/sinking dynamics of biofouled MPs is more complex than can be explained only by SA:V.

5. Conclusion

- According to *in situ* biofouling incubation of natural floating MP particles simulated in this study, not only MPs with densities slightly less than water (such as PE and PP) sink due to biofouling in a short time, but small sized (~100 μm) EPS MPs with a density much less than water also began sinking after 2 weeks of biofouling in an eutrophic river.
- The paradigm of smaller particles sinking faster than larger particles was demonstrated to be applicable to granular MPs of the same polymer type with sizes down to 100 μm.
- There was no significant effect on sinking time/rates between biofouled PE MPs with the same volume but different shapes (and SA:V) in our study, suggesting that other factors, such as the drag coefficient, also play an important role in regulating the floating/sinking dynamics of biofouled MPs.
- Our study demonstrates the importance of biofouling in regulating the sinking of MPs, which supports the role of MP sedimentation as an important mechanism contributing to the "missing" MP stocks in the ocean surface, and thereby affecting the estimation of the global fate and ecosystem risks of plastic debris in aquatic environments.

Declaration of Competing Interest

The authors declare that they have no known competing financial interests or personal relationships that could have appeared to influence the work reported in this paper.

Acknowledgments

This work was supported by the Second Tibetan Plateau Scientific Expedition and Research Program (STEP) (No. 2019QZKK0903), the National Natural Science Foundation of China (Nos. 40906072, 51979197), Public Welfare Technology Research Program of Zhejiang Province (LGF20C030003).

Supplementary materials

Supplementary material associated with this article can be found, in the online version, at doi:10.1016/j.watres.2022.118656.

References

Amaral-Zettler, L.A., Zettler, E.R., Mincer, T.J., Klaassen, M.A., Gallager, S.M., 2021. Biofouling impacts on polyethylene density and sinking in coastal waters: a macro/micro tipping point? Water Res. 201, 117289.
Andrady, A.L., 2011. Microplastics in the marine environment. Mar. Pollut. Bull. 62 (8), 1596–1605.
Andrady, A.L., 2017. The plastic in microplastics: a review. Mar. Pollut. Bull. 119 (1), 12–22.
Artham, T., Sudhakar, M., Venkatesan, R., Madhavan Nair, C., Murty, K.V.G.K., Doble, M., 2009. Biofouling and stability of synthetic polymers in sea water. Int. Biodeterior. Biodegrad. 63 (7), 884–890.
Ballent, A., Corcoran, P.L., Madden, O., Helm, P.A., Longstaffe, F.J., 2016. Sources and sinks of microplastics in Canadian Lake Ontario nearshore, tributary and beach sediments. Mar. Pollut. Bull. 110 (1), 383–395.
Chen, X., Xiong, X., Jiang, X., Shi, H., Wu, C., 2019. Sinking of floating plastic debris caused by biofilm development in a freshwater lake. Chemosphere 222, 856–864.
Cole, M., Lindeque, P.K., Fileman, E., Clark, J., Lewis, C., Halsband, C., Galloway, T.S., 2016. Microplastics alter the properties and sinking rates of zooplankton faecal pellets. Environ. Sci. Technol. 50 (6), 3239–3246.
Cooksey, K.E., Wigglesworth-Cooksey, B., 1995. Adhesion of bacteria and diatoms to surfaces in the sea: a review. Aquat. Microb. Ecol. 9, 87–96.
Cózar, A., Echevarría, F., González-Gordillo, J.I., Irigoien, X., Ubeda, B., Hernández-León, S., Palma, A.T., Navarro, S., García-de-Lomas, J., Ruiz, A., Fernández-de-Puelles, M.L., Duarte, C.M., 2014. Plastic debris in the open ocean. Proc. Natl. Acad. Sci. 111 (28), 10239–10244.
Cózar, A., Martí, E., Duarte, C.M., García-de-Lomas, J., van Sebille, E., Ballatore, T.J., Eguíluz, V.M., González-Gordillo, J.I., Pedrotti, M.L., Echevarría, F., Troublè, R., Irigoien, X., 2017. The Arctic Ocean as a dead end for floating plastics in the North Atlantic branch of the thermohaline circulation. Sci. Adv. 3 (4), e1600582.
Crowe, C.T., 2005. Multiphase Flow Handbook. CRC Press, Boca Raton, New York, p. 1156.
Efimova, I., Bagaeva, M., Bagaev, A., Kileso, A., Chubarenko, I.P., 2018. Secondary microplastics generation in the sea swash zone with coarse bottom sediments: laboratory experiments. Front. Mar. Sci. 5, 313.
El Hadri, H., Gigault, J., Maxit, B., Grassl, B., Reynaud, S., 2020. Nanoplastic from mechanically degraded primary and secondary microplastics for environmental assessments. NanoImpact 17, 100206.
Fazey, F.M., Ryan, P.G., 2016. Biofouling on buoyant marine plastics: an experimental study into the effect of size on surface longevity. Environ. Pollut. 210, 354–360.
Foekema, E.M., De Gruijter, C., Mergia, M.T., van Franeker, J.A., Murk, A.J., Koelmans, A.A., 2013. Plastic in north sea fish. Environ. Sci. Technol. 47 (15), 8818–8824.
Harrison, J.P., Schratzberger, M., Sapp, M., Osborn, A.M., 2014. Rapid bacterial colonization of low-density polyethylene microplastics in coastal sediment microcosms. BMC Microbiol. 14, 232.
Jambeck, J.R., Geyer, R., Wilcox, C., Siegler, T.R., Perryman, M., Andrady, A., Narayan, R., Law, K.L., 2015. Plastic waste inputs from land into the ocean. Science 347 (6223), 768–771.
Ji, X., Ma, Y., Zeng, G., Xu, X., Mei, K., Wang, Z., Chen, Z., Dahlgren, R., Zhang, M., Shang, X., 2021. Transport and fate of microplastics from riverine sediment dredge piles: implications for disposal. J. Hazard. Mater. 404, 124132. Pt A.
Kaiser, D., Kowalski, N., Waniek, J.J., 2017. Effects of biofouling on the sinking behavior of microplastics. Environ. Res. Lett. 12, 124003.
Kane, I.A., Clare, M.A., Miramontes, E., Wogelius, R., Rothwell, J.J., Garreau, P., Pohl, F., 2020. Seafloor microplastic hotspots controlled by deep-sea circulation. Science 368 (6495), 1140–1145.
Kerr, A., Cowling, M.J., 2003. The effects of surface topography on the accumulation of biofouling. Philos. Mag. 83, 2779–2795.
Koelmans, A.A., Kooi, M., Law, K.L., van Sebille, E., 2017. All is not lost: deriving a top-down mass budget of plastic at sea. Environ. Res. Lett. 12 (11), 1–9.
Kooi, M., Nes, E.H.V., Scheffer, M., Koelmans, A.A., 2017. Ups and downs in the ocean: effects of biofouling on vertical transport of microplastics. Environ. Sci. Technol. 51 (14), 7963–7971.
Lagarde, F., Olivier, O., Zanella, M., Daniel, P., Hiard, S., Caruso, A., 2016. Microplastic interactions with freshwater microalgae: hetero-aggregation and changes in plastic density appear strongly dependent on polymer type. Environ Pollut. 215, 331–339.
Leiser, R., Wu, G.M., Neu, T.R., Wendt-Potthoff, K., 2020. Biofouling, metal sorption and aggregation are related to sinking of microplastics in a stratified reservoir. Water Res. 176, 115748.
Leiser, R., Schumann, M., Dadi, T., Wendt-Potthoff, K., 2021. Burial of microplastics in freshwater sediments facilitated by iron-organo flocs. Sci. Rep. 11, 24072.
Lobelle, D., Cunliffe, M., 2011. Early microbial biofilm formation on marine plastic debris. Mar. Pollut. Bull. 62 (1), 197–200.
Long, M., Moriceau, B., Gallinari, M., Lambert, C., Huvet, A., Raffray, J., Soudant, P., 2015. Interactions between microplastics and phytoplankton aggregates: impact on their respective fates. Mar. Chem. 175, 39–46.
Mani, T., Primpke, S., Lorenz, C., Gerdts, G., Burkhardt-Holm, P., 2019. Microplastic pollution in benthic midstream sediments of the Rhine river. Environ. Sci. Technol. 53 (10), 6053–6062.
Mei, K., Liao, L., Zhu, Y., Lu, P., Wang, Z., Dahlgren, R.A., Zhang, M., 2014. Evaluation of spatial-temporal variations and trends in surface water quality across a rural-suburban-urban interface. Environ. Sci. Pollut. Res. Int. 21 (13), 8036–8051.
Miao, L., Gao, Y., Adyel, T.M., Huo, Z., Liu, Z., Wu, J., Hou, J., 2021. Effects of biofilm colonization on the sinking of microplastics in three freshwater environments. J. Hazard. Mater. 413, 125370.
Michels, J., Stippkugel, A., Lenz, M., Wirtz, K., Engel, A., 2018. Rapid aggregation of biofilm-covered microplastics with marine biogenic particles. Proc. R. Soc. B 285, 20181203.
Murga, R., Stewart, P.S., Daly, D., 1995. Quantitative analysis of biofilm thickness variability. Biotechnol. Bioeng. 45 (6), 503–510.
Nava, V., Matias, M.G., Castillo-Escrivà, A., Messyasz, B., Leoni, B., 2021. Microalgae colonization of different microplastic polymers in experimental mesocosms across an environmental gradient. Glob. Chang. Biol. 28, 1402–1413.
Oberbeckmann, S., Labrenz, M., 2020. Marine microbial assemblages on microplastics: diversity, adaptation, and role in degradation. Ann. Rev. Mar. Sci. 12, 209–232.
Padisák, J., Soróczki-Pintér, É., Rezner, Z., 2003. Sinking properties of some phytoplankton shapes and the relation of form resistance to morphological diversity of plankton - an experimental study. Hydrobiologia 500, 243–257.
Parrish, K., Fahrenfeld, N.L., 2019. Microplastic biofilm in fresh- and wastewater as a function of microparticle type and size class. Environ. Sci. Water Res. Technol. 2019 (5), 495–505.
Reisser, J., Slat, B., Noble, K., Plessis, K.D., Epp, M., Proietti, M., de Sonneville, J., Becker, T., Pattiaratchi, C., 2015. The vertical distribution of buoyant plastics at sea: an observational study in the North Atlantic gyre. Biogeosciences 12 (4), 1249–1256.
Rochman, C.M., Hoellein, T., 2020. The global odyssey of plastic pollution. Science 368 (6496), 1184–1185.
Rummel, C.D., Jahnke, A., Gorokhova, E., Khünel, D., Schmitt-Jansen, M., 2017. Impacts of biofilm formation on the fate and potential effects of microplastic in the aquatic environment. Environ. Sci. Technol. Lett. 4, 258–267.

Ryan, P.G., 2015. Does size and buoyancy affect the long-distance transport of floating debris? Environ. Res. Lett. 10, 084019.
Sagawa, N., Kawaai, K., Hinata, H., 2018. Abundance and size of microplastics in a coastal sea: comparison among bottom sediment, beach sediment, and surface water. Mar. Pollut. Bull. 133, 532–542.
Semcesen, P.O., Wells, M.G., 2021. Biofilm growth on buoyant microplastics leads to changes in settling rates: implications for microplastic retention in the Great Lakes. Mar. Pollut. Bull. 170, 112573.
Smith, I.L., Stanton, T., Law, A., 2021. Plastic habitats: algal biofilms on photic and aphotic plastics. J. Hazard. Mater. Lett. 2, 100038.
Thompson, R.C., Olsen, Y., Mitchell, R.P., Davis, A., Rowland, S.J., John, A.W., McGonigle, D., Russell, A.E., 2004. Lost at sea: where is all the plastic? Science 304 (5672), 838.
Tu, C., Chen, T., Zhou, Q., Liu, Y., Wei, J., Waniek, J.J., Luo, Y., 2020. Biofilm formation and its influences on the properties of microplastics as affected by exposure time and depth in the seawater. Sci. Total Environ. 734, 139237.
Tu, C., Liu, Y., Li, L., Li, Y., Vogts, A., Luo, Y., Waniek, J.J., 2021. Structural and functional characteristics of microplastic associated biofilms in response to temporal dynamics and polymer types. Bull. Environ. Contam. Toxicol. 107 (4), 633–639.
Turner, A., 2020. Foamed polystyrene in the marine environment: sources, additives, transport, behavior, and impacts. Environ. Sci. Technol. 54 (17), 10411–10420.
Van Melkebeke, M., Janssen, C., De Meester, S., 2020. Characteristics and sinking behavior of typical microplastics including the potential effect of biofouling: implications for remediation. Environ. Sci. Technol. 54 (14), 8668–8680.
Vaughan, R., Turner, S.D., Rose, N.L., 2017. Microplastics in the sediments of a UK urban lake. Environ. Pollut. 229, 10–18.
Wang, Z., Su, B., Xu, X., Di, D., Huang, H., Mei, K., Dahlgren, R.A., Zhang, M., Shang, X., 2018. Preferential accumulation of small (<300 μm) microplastics in the sediments of a coastal plain river network in eastern China. Water Res. 144, 393–401.
Weiss, L., Ludwig, W., Heussner, S., Canals, M., Ghiglione, J.F., Estournel, C., Constant, M., Kerhervé, P., 2021. The missing ocean plastic sink: gone with the rivers. Science 373 (6550), 107–111.
Woodall, L.C., Sanchez-Vidal, A., Canals, M., Paterson, G.L., Coppock, R., Sleight, V., Calafat, A., Rogers, A.D., Narayanaswamy, B.E., Thompson, R.C., 2014. The deep sea is a major sink for microplastic debris. R. Soc. Open Sci. 1 (4), 140317.
Wright, R.J., Erni-Cassola, G., Zadjelovic, V., Latva, M., Christie-Oleza, J.A., 2020. Marine plastic debris: a new surface for microbial colonization. Environ. Sci. Technol. 54 (19), 11657–11672.
Yang, L., Zhang, Y., Kang, S., Wang, Z., Wu, C., 2021. Microplastics in freshwater sediment: a review on methods, occurrence, and sources. Sci. Total Environ. 754, 141948.
Yao, W.M., Di, D., Wang, Z.F., Liao, Z.L., Huang, H., Mei, K., Dahlgren, R.A., Zhang, M. H., Shang, X., 2019. Micro- and macroplastic accumulation in a newly formed *Spartina alterniflora* colonized estuarine saltmarsh in southeast China. Mar. Pollut. Bull. 149, 110636.
Ye, S., Andrady, A.L., 1991. Fouling of floating plastic debris under Biscayne Bay exposure conditions. Mar. Pollut. Bull. 22, 608–613.